5-2-2016

Large extinction ratio optical electrowetting shutter.

Ryan D Montoya
University of Colorado Boulder

Kenneth Underwood
University of Colorado Boulder

Soraya Terrab
University of Colorado Boulder

Alexander M Watson
University of Colorado Boulder

Victor M Bright
University of Colorado Boulder

See next page for additional authors

Authors
Ryan D Montoya, Kenneth Underwood, Soraya Terrab, Alexander M Watson, Victor M Bright, and Juliet T Gopinath

Large extinction ratio optical electrowetting shutter

Ryan D. Montoya,[1,*] Kenneth Underwood,[2] Soraya Terrab,[3] Alexander M. Watson,[3] Victor M. Bright,[3] and Juliet T. Gopinath[1,2]

[1]*Department of Electrical, Computer, and Energy Engineering, University of Colorado, Boulder, Colorado, 80309, USA*

[2]*Department of Physics, University of Colorado, Boulder, Colorado, 80309, USA*

[3]*Department of Mechanical Engineering, University of Colorado, Boulder, Colorado, 80309, USA*

[*]*ryan.montoya@colorado.edu*

Abstract: A large extinction ratio optical shutter has been demonstrated using electrowetting liquids. The device is based on switching between a liquid-liquid interface curvature that produces total internal reflection and one that does not. The interface radius of curvature can be tuned continuously from 9 mm at 0 V to −45 mm at 26 V. Extinction ratios from 55.8 to 66.5 dB were measured. The device shows promise for ultracold chip-scale atomic clocks.

OCIS codes: (230.0230) Optical devices; (110.1080) Active or adaptive optics; (080.3630) Lenses.

References and links

1. J. Huo, K. Liu, and X. Chen, "1 x 2 precise electro-optic switch in periodically poled lithium niobate," Opt. Express **18**(15), 15603–15608 (2010).
2. W. J. Schwenger and J. M. Higbie, "High-speed acousto-optic shutter with no optical frequency shift," Rev. Sci. Instrum. **83**(8), 083110 (2012).
3. H. Veladi, R. R. A. Syms, and H. Zou, "Low power, high extinction electrothermal MEMS iris VOA," Proc. SPIE **6186**, 61860J (2006).
4. A. Braslau, M. Deutsch, P. S. Pershan, A. H. Weiss, J. Als-Nielsen, and J. Bohr, "Surface roughness of water measured by x-ray refelctivity," Phys. Rev. Lett. **54**(2), 114–117 (1985).
5. L. Li, C. Liu, and Q. H. Wang, "Optical switch based on tunable aperture," Opt. Lett. **37**(16), 3306–3308 (2012).
6. H. Ren, S. Xu, and S.-T. Wu, "Optical switch based on variable aperture," Opt. Lett. **37**(9), 1421–1423 (2012).
7. D.-Y. Zhang, V. Lien, Y. Berdichevsky, J. Choi, and Y.-H. Lo, "Fluidic adaptive lens with high focal length tunability," Appl. Phys. Lett. **82**(19), 3171 (2003).
8. L. Dong, A. K. Agarwal, D. J. Beebe, and H. Jiang, "Adaptive liquid microlenses activated by stimuli-responsive hydrogels," Nature **442**(7102), 551–554 (2006).
9. A. Schultz, J. Heikenfeld, H. S. Kang, and W. Cheng, "1000:1 contrast ratio transmissive electrowetting displays," J. Disp. Technol. **7**(11), 583–585 (2011).
10. C.-C. Yu, J.-R. Ho, and J.-W. J. Cheng, "Tunable liquid iris actuated using electrowetting effect," Opt. Eng. **53**(5), 057106 (2014).
11. J. Heikenfeld and A. J. Steckl, "High-transmission electrowetting light valves," Appl. Phys. Lett. **86**(15), 151121 (2005).
12. C. Liu, L. Li, and Q.-H. Wang, "Bidirectional optical switch based on electrowetting," J. Appl. Phys. **113**(19), 193106 (2013).
13. P. Müller, D. Kopp, A. Llobera, and H. Zappe, "Optofluidic router based on tunable liquid-liquid mirrors," Lab Chip **14**(4), 737–743 (2014).
14. C. Liu, D. Wang, L.-X. Yao, L. Li, and Q.-H. Wang, "Electrowetting-actuated optical switch based on total internal reflection," Appl. Opt. **54**(10), 2672–2676 (2015).
15. C. U. Murade, D. van der Ende, and F. Mugele, "High speed adaptive liquid microlens array," Opt. Express **20**(16), 18180–18187 (2012).
<jrn>16. S. Terrab, A. M. Watson, C. Roath, J. T. Gopinath, and V. M. Bright, "Adaptive electrowetting lens-prism element," Opt. Express **23**(20), 25838–25845 (2015).</jrn>
<jrn>17. M. Frieder and J.-C. Baret, "Electrowetting: from basics to applications," J. Phys. Condens. Matter **17**(28), R705–R774 (2005).</jrn>

#259955 Received 24 Feb 2016; revised 6 Apr 2016; accepted 6 Apr 2016; published 25 Apr 2016

1. Introduction

High extinction ratio optical shutters are important for atomic clocks, gyroscopes, communications, lab-on-a-chip systems, and displays. Existing technologies include integrated lithium-niobate electro-optic modulators [1], acousto-optic modulators [2], and mechanical methods based on diaphragms or blades [3]. These systems provide elegant solutions for many applications. However, integrated modulators suffer from limited aperture and contrast ratio, acousto-optic modulators are constrained in their extinction ratio by scattering, and mechanical methods are prone to friction issues and long term wear. An attractive alternative for applications requiring large extinction ratio without mechanical parts is offered by liquid-based optical devices. Liquids have well defined interfaces, angstrom level surface roughness [4], optical isotropy, and low optical loss. A variety of techniques exist for controlling liquids including electrowetting [5], dielectrophoresis [6], pressure driven elastic membranes [7], and hydrogels [8]. The electrowetting effect is appealing as it enables transmissive, compact devices with minimal voltage requirements and no mechanical parts. The technique has been used to demonstrate lens and prism arrays for displays, imaging, tunable apertures and switches [5–16].

Although there are previous demonstrations of electrowetting-based displays [9], tunable irises [10], and switches [11–14], high extinction ratio (beyond 30 dB) shutters have not been demonstrated. There are many implementations of these functionalities, using opaque ink or oil droplets [5, 9, 11], tunable irises, and liquid interfaces operating around total internal reflection [14] (TIR). In contrast, the shutter reported here demonstrates 66 dB of extinction ratio and low voltage operation due to high quality materials and a unique geometry. To the best of our knowledge, this is the largest extinction ratio demonstrated by an electrowetting-based total-internal-reflection device to date.

2. Shutter design

The optical shutter is based on the principle of electrowetting, in which the contact angle and shape of a liquid droplet or interface is controlled with an applied voltage. In this design, the curvature of the liquid interface allows the device to switch between total internal reflection and transmission, as illustrated in Fig. 1. The device consists of a sealed glass cylinder that is filled with two liquids, dodecane oil and water, and a prism to couple in the incident light at the correct angle. The sidewall of the cylinder has a thin film electrode followed by a dielectric layer and a hydrophobic coating. The cylinder is thermally bonded with glass frit to a glass substrate, with a platinum bottom electrode placed in between the cylinder and substrate. At 0 V, incoming light strikes the liquid interface at approximately 72°, 4 degrees beyond the water-oil TIR critical angle of 68°, relative to the surface normal. Electrically tuning the interface curvature causes incident light at an appropriate angle and offset from the center to cross this critical angle and switch between total internal reflection and transmission states.

#259955 Received 24 Feb 2016; revised 6 Apr 2016; accepted 6 Apr 2016; published 25 Apr 2016

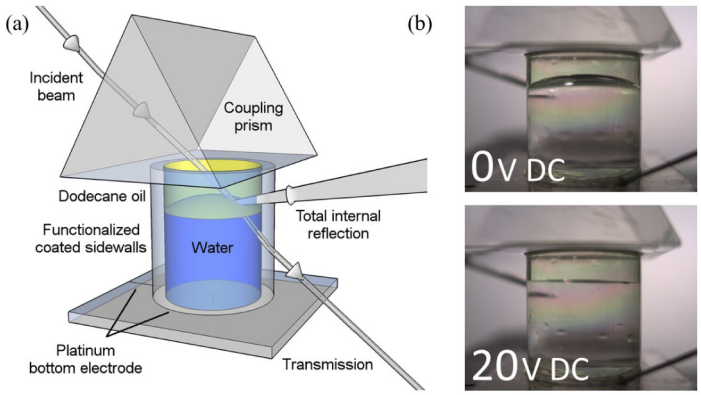

Fig. 1. (IZO) Indium zinc oxide a) Design for shutter, based on an electrowetting lens in glass tube. By changing the applied voltage, the lens radius can switch from 9 mm to –45 mm. b) A glass substrate with platinum electrode is bonded with glass frit to a tube coated with IZO (300 nm), Parylene C dielectric (1 μm) and Teflon AF 1600 hydrophobic layer (100 nm). The photographs show a shutter device at 0 V with an initial lens radius of 9 mm and at 20 V with an infinite radius of curvature.

3. Fabrication

We implement the electrowetting shutter using a design that enables tuning of the curvature of an interface between polar (water with 1% sodium dodecyl sulfate) and non-polar (dodecane oil) liquids. A diagram of the device is shown in Fig. 1(a), while a photo of a fabricated device in operation is shown in Fig. 1(b).

The fabrication steps of the liquid shutter device are illustrated in Fig. 2. Glass frit solution is placed on the rim of a glass tube and baked at 400 °C [Fig. 2(a)]. A platinum wire is annealed and shaped in the form of a loop and serves as the base electrode. The wire is aligned onto the glass base underneath the glass tube, with glass frit facing down toward the substrate. The tube is clamped down to the substrate and the fixture is cured at 550 °C to allow the frit to bond the glass pieces together, resulting in a hermetic seal between the tube and base [Figs. 2(c)-2(d)].

The platinum wire and base of the tube are masked off, with Kapton tape on the outer tube shell and substrate and a Teflon plug inside the tube, before the sides of the tube are sputter-coated with indium zinc oxide (IZO) to form a continuous film from the inside to the outside of the tube. IZO, an optically transparent conductor, is sputtered onto the sample at an argon pressure of 5 mTorr and power of 120 W to achieve a deposition thickness of 300 nm. The mean free path of the sputtered IZO in the argon at this pressure is an order of magnitude shorter than the distance between target and substrate, enabling diffuse sputtering and a conformal coating from inside to outside of the tube.

Before depositing the thin film dielectric, the glass tube is cleaned and the exterior masked with Kapton tape to allow electrode contact from outside the tube after the dielectric deposition. Parylene C is deposited in a vapor-phase, low-vacuum system by VSI Parylene to a thickness of 0.93 μm. The samples are then dip-coated in a 1:20 solution of Dupont's Teflon AF 1600: Fluorinert FC-40 for the 100 nm hydrophobic coating. To cure the Teflon above its glass transition temperature of 165°C, the samples are heated in an oven at 120 °C for 10 min and then 170 °C for 20 min. The insets in Figs. 2(e)-2(f) show the thin film layers on the device.

#259955 Received 24 Feb 2016; revised 6 Apr 2016; accepted 6 Apr 2016; published 25 Apr 2016

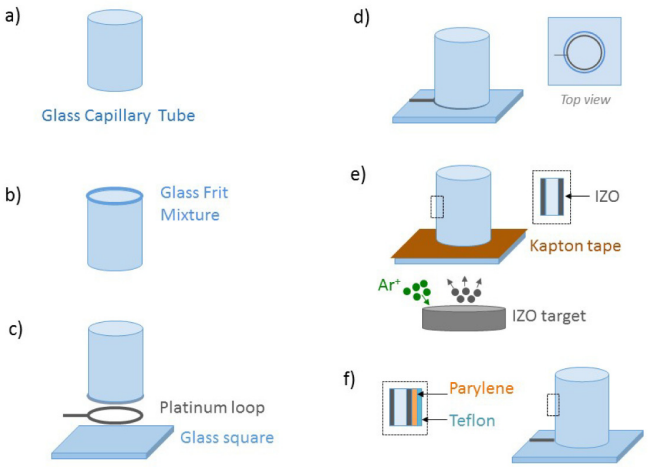

Fig. 2. Fabrication of the optical shutter devices. (a) We start with a glass tube and glass substrate. (b-d) A platinum wire is placed between the tube and substrate, and glass frit is used to bond the two together. (e) The substrate is masked with Kapton tape outside the tube and a Teflon plug inside the tube. The glass tube is coated with indium zinc oxide (IZO). (f) The assembled tubes are coated with Parylene dielectric (VSI Parylene) and finished inside with a dip coat of Teflon AF hydrophobic layer.

The devices are filled with a 1% sodium dodecyl sulfate (SDS, Sigma-Aldrich) in DI water solution. In addition to reducing the surface tension between the polar liquid and oil, the SDS provides a large, negatively charged dodecyl sulfate ion, which cannot easily penetrate the Parylene layer when a positive DC voltage is applied to the sidewalls. The dodecane oil is then injected into the device to form the oil/water electrowetting-tunable interface.

4. Results

We characterized the extinction ratio, the contact angle as a function of voltage, and the response time. The response time and extinction ratio were measured using a 780 nm laser diode in the optical setup shown in Fig. 3. The laser diode is spatially filtered and focused to a 250 μm diameter spot on the liquid interface, offset from the center of the device by 2-3 mm to optimize the incident light position for switching between transmission and total internal reflection. In the case of the transmitted beam, the output light is collimated and focused through two spatial filters of pinhole diameters of 100 and 75 μm. For the totally internally reflected beam, one 200 μm pinhole is used. Spatial filters were selected to provide maximum extinction ratio for both the transmitted and internally reflected states.

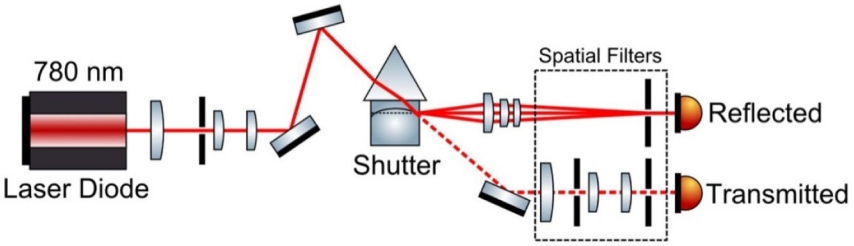

Fig. 3. Optical setup for measuring extinction ratio and response time of the shutter. The 780 nm laser diode is spatially filtered and then focused by a long focal length lens to minimize spot size incident on the liquid-liquid interface. The correct angle of incidence is achieved using a pair of mirrors. Both the transmitted and totally internally reflected beam states are then passed through respective spatial filters to photodetectors.

#259955 Received 24 Feb 2016; revised 6 Apr 2016; accepted 6 Apr 2016; published 25 Apr 2016

The extinction ratio was measured by collecting the light onto two silicon photodetectors that are connected to either an oscilloscope or a lock-in amplifier. The results of the extinction measurements are shown in Fig. 4(a). We measure an extinction ratio of 55.8 dB for the beam that is transmitted through the device ($P_{trans,25V} / P_{trans,OV}$), and 66.5 dB for the beam that undergoes total internal reflection ($P_{tir,0V} / P_{tir,25V}$). This is currently the highest extinction ratio measured from an electrowetting optical shutter to the best of our knowledge. A sharp change in the transmitted optical power can be seen in Fig. 4(a) at ~20 V. This behavior was also observed by imaging the beam with a camera after the first spatial filter. Due to the device geometry, reflections and sidewall scattering change dramatically as a function of voltage (contact angle). Two spatial filters are sufficient to eliminate most of the undesirable changes. However, at 20 V, a local peak arises as a spurious beam passes through both spatial filters before being blocked at voltages greater than 20 V. This change can be mitigated by minimizing sidewall scattering and reflections with antireflection coatings and changes in the device geometry. MATLAB modeling of the device including secondary reflections can be seen in Fig. 4(b). The model qualitatively matches the shape of the experimental results and quantitatively confirms the maximum extinction ratio at 0 V and ~25 V for the internally reflected beam. The model does not capture scattering, and so demonstrates lower minimum power in the transmitted branch. At ~24 V, no power is received in the MATLAB model. Discrepancies between experiment and model may be attributable to error for the following reasons: (1) the 3D device is simplified into a 2D model, (2) many experimental parameters can only be estimated and the system is sensitive to small changes, and (3) the model does not include scattering.

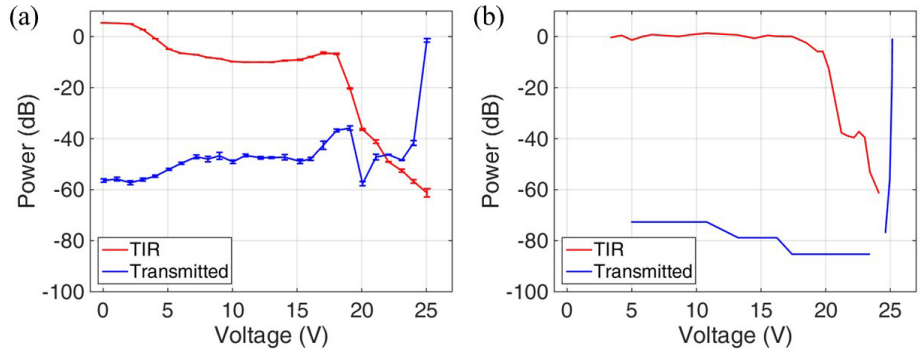

Fig. 4. Total internal reflection (TIR) a) TIR and transmitted beam detected optical power versus applied voltage. The TIR beam exhibits 66 dB of extinction ratio. b) TIR and transmitted beam MATLAB theoretical results.

The contact angle of the liquid interface was characterized by analyzing photographs of the device as a function of applied voltage. The resulting curvature of the liquid interface can be fit to the Lippmann-Young equation [17]. Figure 5 illustrates the contact angle vs. applied voltage. The shaded region indicates the region of reflection for an angle of incidence of the incident beam (relative to the liquid normal) that exceeds 68 degrees, the critical angle.

#259955 Received 24 Feb 2016; revised 6 Apr 2016; accepted 6 Apr 2016; published 25 Apr 2016

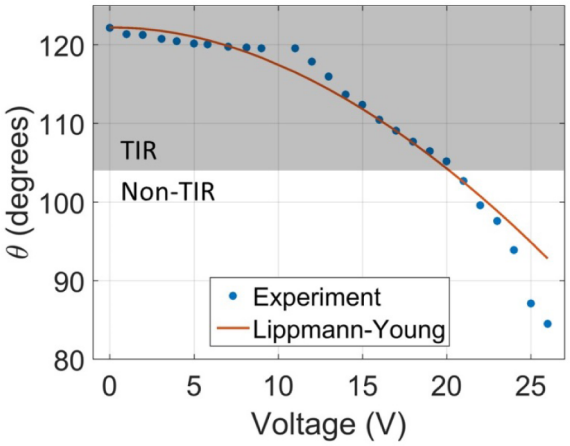

Fig. 5. Contact angle vs. voltage of curved interface. The shaded area indicates where total internal reflection (TIR) can be achieved with our setup. The non-TIR region indicates where none of the incident beam is internally reflected.

From 0 V to ~18 V, the device operates in the total internal reflection state, as seen in the shaded area of Fig. 5. This agrees well with the extinction measurements in Fig. 4(a); both the reflected and transmitted beams exhibit relatively small changes in optical power until the applied voltage exceeds ~18 V. As the device enters the non-TIR state, the reflected beam power drops sharply, followed by a rise in the transmitted power as the beam becomes aligned to the spatial filter system. The reflected beam power remains high until the ~18 V transition as some of the incident beam is internally reflected at this interval. However, the two spatial filter systems in the transmitted branch require very specific alignment to receive significant power, and it is not until the curvature has approached −45 mm radius that significant power is detected.

The system response time was measured by collecting incident power vs. time on the transmitted optical power detector in response to a 26 V step function. For 90% transmission, the overall response time of the system was measured to be 4.88 seconds. Simulation however suggests that the response time of the liquid interface is approximately 300 ms to achieve 95% curvature. The system is highly sensitive to small changes in the height and curvature of the liquid interface due to alignment through the spatial filters, necessitating a much longer settling time to detect appreciable transmitted power. From the experimental results, the curvature of the interface must exceed 99% of the long-term curvature before we reach 90% optical transmission, and the low-velocity of the liquid near this steady state curvature increases the shutter response time. The application of spatial filters on the output beams is necessitated by the scattering produced via sidewall interaction, however the use of spatial filters significantly decreases the acceptance angle for alignment and therefore limits the transmission state to above 99% curvature. If the scattering can be reduced, the spatial filters can be tuned to allow transmission for a wider range of curvatures. This will have significant effect on the response time as the curvature according to simulation should reach 95% curvature a full order of magnitude faster than 99% curvature. Furthermore, no power oscillations were observed as the device approached maximum curvature, suggesting that the system is overdamped. The overall response time is therefore limited for the following reasons: (1) The system is highly sensitive to small changes in curvature (2) the device has a large liquid volume (3) the system is overdamped. By using a smaller device design in the future and further reducing scattering, it should be possible to ensure millisecond response times from this shutter [15].

#259955 Received 24 Feb 2016; revised 6 Apr 2016; accepted 6 Apr 2016; published 25 Apr 2016

The ultrasmooth, angstrom-level surface roughness at the liquid-liquid interface gives the device design the potential for higher extinction ratios if the secondary reflections and sidewall interactions can be avoided. Future designs could mitigate the effects of secondary reflections and scattering by using anti-reflection coatings. Scattering effects can be mitigated with new geometries to avoid interaction with solid interfaces such as the coated sidewalls. Furthermore, existing electrowetting prism designs [16] can further reduce the effects of secondary reflections and scattering by altogether avoiding interaction with curved liquid-liquid interfaces, instead biasing the TIR state on a flat, angled liquid interface. This has the potential to further increase the extinction ratio. Future system response time may also benefit from biasing the device operation around the transition point of total internal reflection and transmission, taking advantage of the full extinction ratio while reducing necessary changes in contact angle.

5. Conclusion

In summary, we have demonstrated a high extinction ratio optical shutter based on an electrowetting lens. The smooth interface between the liquids combined with operation based on total internal reflection enables a high extinction ratio of 55 and 66 dB for the transmitted and reflected beams, respectively. Future designs may achieve even greater extinction by avoiding sidewall interaction as well as utilizing new geometries, and with future miniaturization show promise for high speed shutter applications in atomic physics, displays, communications and imaging.

Acknowledgments

The authors would like to acknowledge technical assistance from Kevin Dease, Omkar Supekar, Dr. Joseph Brown, and Dr. Mohammed Zohrabi (University of Colorado Boulder). We are also grateful for technical discussions with Dr. Andrew Jones (Lockheed Martin Aculight). We are grateful to Christopher Roath of VSI Parylene for performing the Parylene deposition. We would also like to thank Yehor Novikov with the Research Glassblowing Shop at the Cooperative Institute for Research in Environmental Sciences (CIRES) for assistance with glass tube fabrication. The authors acknowledge funding support from the Butcher Foundation, National Science Foundation (NSF) IDBR DBI-1353757, and DARPA MTO W31P4Q-14-1-0006, under the CAMS program.

#259955 Received 24 Feb 2016; revised 6 Apr 2016; accepted 6 Apr 2016; published 25 Apr 2016